Electrical Properties of Co-Doped Ceria Electrolyte $Ce_{0.8-x}Gd_{0.2}Sr_xO_{2-\delta}$ $(0.0 \leq x \leq 0.1)$

S. Ramesh and C. Vishnuvardhan Reddy*
Department of Physics, University College of Science, Osmania University
Hyderabad, 500 007 India

(Received January 30, 2009; in final form March 30, 2009)

Effects of strontium doping on electrical properties of gadolinium-doped ceria were investigated. The $Ce_{0.8-x}Gd_{0.2}Sr_xO_{2-\delta}$ $(0.0 \leq x \leq 0.1)$ compositions were prepared by sol-gel method and sintered at 1300°C for 8 h, the bulk densities were over 93% of theoretical density. These results were consistent with scanning electron microscope. The crystallite size of these materials was determined using the X-ray powder diffractometer and the sizes range from 19.4 nm to 24.4 nm. From the experimental results, it was observed that the composition $Ce_{0.8-x}Gd_{0.2}Sr_xO_{2-\delta}$ $(x = 0.02)$ exhibits higher conductivity $(23.6 \times 10^{-3}$ S cm$^{-1})$ and minimum activation energy (0.83 eV) at 700°C. This composition is thus a potential candidate for use as electrolyte applications in intermediate temperature solid oxide fuel cells.

PACS numbers: 65.40.De, 66.10.Ed, 81.20.Fw, 82.45.Gj, 82.47.Ed, 82.45.Xy

1. Introduction

Solid oxide fuel cells (SOFC) have the ability to provide electrical energy with high efficiency and low environmental impact. There are different types of solid oxide fuel cell electrolytes like solid oxide electrochemical cells [1, 2] and solid oxide fuel cells [3], of these tetragonal or cubic yttrium stabilized zirconia (YSZ) is the most common electrolyte used in commercial SOFC's [4, 5]. YSZ exhibits highest ionic conductivity at 1000°C, hence it requires high operating temperatures.

Doped ceria oxides shown much higher ionic conductivity at relatively low temperatures (500–800°C) in comparison to that of YSZ and have been extensively studied as most promising electrolyte materials for intermediate temperature solid oxide fuel cells (IT-SOFC). Among the various dopants studied, gadolinia doped ceria (GDC) and samarium doped ceria (SDC) have been reported to have the highest ionic conductivity [6]. However, there have been some contradictions in the literature concerning which of the two is better. Steele [7] and Van Herle et al. [8, 9] reported that GDC showed higher ionic conductivity, whereas the reverse results were reported in the literature [10]. This disagreement probably results from divergence in sample preparation. Other than singly doped ceria, many studies have been reported on co-doped samples and results suggest that co-doping may enhance conductivity even at moderate or intermediate temperatures [11–14].

* corresponding author; e-mail: reddy_cvv@rediffmail.com

In the present paper, Gd^{3+} and Sr^{2+} co-doped ceria based $Ce_{0.8-x}Gd_{0.2}Sr_xO_{2-\delta}$ $(x = 0.0, 0.02, 0.04, 0.06, 0.08, 0.1)$ materials were prepared and characterized. This paper is intended to study structure and electrical conductivity of the Sr co-doped ceria in comparison with gadolinium doped ceria $(Ce_{0.8}Gd_{0.2}O_{2-\delta})$.

2. Experimental

The samples with the general formula of $Ce_{0.8-x}Gd_{0.2}Sr_xO_{2-\delta}$ (where $x = 0.00, 0.02, 0.04, 0.06, 0.08, 0.1$) were synthesized by sol-gel method. Cerium nitrate hexahydrate $Ce(NO_3)_2 \cdot 6H_2O$, gadolinium oxide (Gd_2O_3) and strontium nitrate $Sr(NO_3)_2$ were used as starting materials. Stoichiometric amounts of cerium nitrate hexahydrate, strontium nitrates were dissolved in distilled water. Gd_2O_3 was converted into nitrate form with the addition of nitric acid and mixed with above solution. Citric acid in the 1:1 molar ratio added to the solution and then the pH was adjusted to $\approx$ 7 with ammonia, adding drop by drop to the solution. Then the solution was placed on magnetic stirrer under continuous stirring at 70°C for 10–13 h and homogeneous sol was formed. Ethylene glycol was added to the solution in the 1:1.2 molar ratio at this stage and heated at 85°C until gel formation. The gel was dried at 75°C, resulting in a light yellow colored ash. Then the ash was decomposed to a polycrystalline oxide by heating to 600°C for 2 h. The oxidation of Ce^{3+} to Ce^{4+} occurred during this stage [7]. The resultant ash was ground in an agate mortar to get a fine homogeneous powder. Then the powders were pelletized using a

stainless steel die of dimensions 10 mm in diameter and approximate 2 mm in thickness, with the help of hydraulic press at 5 MPa and sintered finally at 1300°C for 8 h with a programmed heating rate of 5°C/min. Densities of all sintered samples were measured using the Archimedes principle and were estimated to be 93% of theoretical density or above.

Crystallographic information of the samples was determined using the Pan analytical X'Pert Pro X-ray diffractometer with Cu K_α radiation (1.54056 Å). The crystallite size (D_{XRD}) was calculated according to the Scherrer equation

$$D_{\mathrm{XRD}} = 0.9\lambda/\beta\cos\theta,$$

where λ is the wavelength of the radiation, θ is the diffraction angle, and β is the full width at half maximum.

The microstructure of the sintered pellets was studied using scanning electron microscope (SEM) (FIPL-SEM).

Electrical impedance (Z) and phase angles (θ) were measured as a function of frequency (0.1 kHz–1 MHz) using LCR Hi-Tester (HIOKI 3531Z), Japan on sintered pellet specimens with 10 mm diameter and 2 mm thickness. The conductivity measurements were taken at different temperatures in the range 300–700°C in air. Silver paste coated each side of the sample, which was subsequently dried, producing solid silver electrode on both sides of the pellet.

A complex plane plot, in which real impedance, Z' versus imaginary impedance, Z'' was produced for each set of data. Non-linear curve fitting on these plots, sample resistance R can be obtained. The conductivity σ was then calculated from resistance, thickness l, cross-sectional area A, using Eq. (1)

$$\sigma = \frac{l}{RA}. \tag{1}$$

The activation energy for conduction is obtained by plotting the ionic conductivity data in the Arrhenius relation for thermally activated conduction. Activation energy calculated using Eq. (2),

$$\sigma T = \sigma_0 \exp\left(-\frac{E_a}{kT}\right) \tag{2}$$

where E_{a} is the activation energy for conduction, T is the absolute temperature, k is the Boltzmann constant and σ_0 is a pre-exponential factor. The equation may be linearized by plotting a logarithmic relationship between $\log(\sigma T)$ and $1000/T$.

The main contribution of the conductivity of ceria-based compounds in air is oxide ionic conductivity and that of electronic conductivity, which is negligible [10]. In this paper the conductivity measured in air can be treated as oxide ionic conductivity.

3. Results and discussion

Figure 1 displays the X-ray diffraction (XRD) patterns of strontium co-doped ceria samples with the fluorite structure. Strontium co-doped ceria ceramics sintered at 1300°C show that the powders contain only a cubic fluorite structure with the space group $Fm\bar{3}m$ (ICDD 075-0162). The crystallite sizes of the sample powders were calculated by the Scherrer formula and are in the range 19.4 to 24.4 nm (Table I). The introduction of Sr^{2+} into Ce^{4+} can cause a small shift in the ceria peaks. This shift is indicative of a change in the lattice parameter. The lattice parameter (a) of the co-doped ceria can be calculated using the following relation:

$$d = \lambda/2\sin\theta, \quad a = d\sqrt{h^2+k^2+l^2},$$

where d is the inter planar spacing, λ is the wavelength of the radiation (1.54065 Å), θ is the diffraction angle, and a is the lattice parameter.

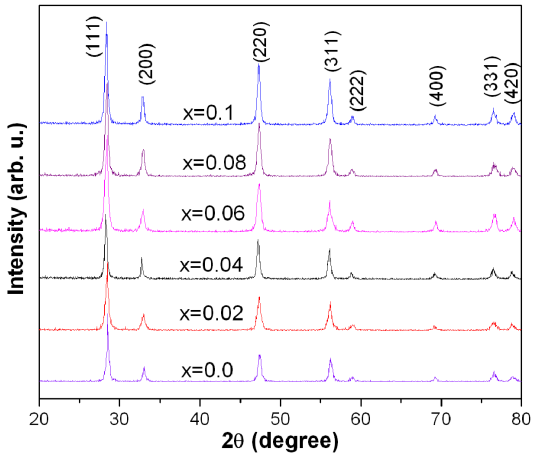

Fig. 1. The XRD patterns of $Ce_{0.8-x}Gd_{0.2}Sr_xO_{2-\delta}$ (x = 0.0–0.1) sintered at 1300°C.

TABLE I

Crystallite size of $Ce_{0.8-x}Gd_{0.2}Sr_xO_{2-\delta}$ series of specimens sintered at 1300°C for 8 h, wherein x = 0.0, 0.02, 0.04, 0.06, 0.08, 0.1.

Composition	Crystallite size [nm]
x = 0.0	24.4
x = 0.02	22.8
x = 0.04	21.9
x = 0.06	21
x = 0.08	20.5
x = 0.1	19.4

The lattice parameter increases linearly with the increase in Sr content. This is due to different ionic radii of Ce^{4+} (0.96 Å) and Sr^{2+}(1.26 Å) [15]. Doping Sr in Ce lattice will induce a uniform strain in the lattice, as the material is elastically deformed. This effect causes the lattice plane spacing to change and the diffraction peaks to shift to a new 2θ position. As the Sr content increases, the lattice constant increases as shown in Ta-

ble II for $Ce_{0.8-x}Gd_{0.2}Sr_xO_{2-\delta}$ (0.0–0.1) ceramic electrolyte materials. This indicates that Sr had dissolved into the Ce sites in $Ce_{0.8-x}Gd_{0.2}Sr_xO_{2-\delta}$ and isostructural phases had been formed.

TABLE II

The lattice parameters and phase structures of $Ce_{0.8-x}Gd_{0.2}Sr_xO_{2-\delta}$ series of specimens sintered at 1300°C for 8 h, wherein x = 0.0, 0.02, 0.04, 0.06, 0.08, 0.1.

Composition	Lattice parameter [Å]	Volume [Å^3]	Structure
x = 0.0	5.423	159.484	Cubic
x = 0.02	5.427	159.837	Cubic
x = 0.04	5.434	160.457	Cubic
x = 0.06	5.439	160.900	Cubic
x = 0.08	5.446	161.522	Cubic
x = 0.1	5.452	162.056	Cubic

The microstructure of the sintered pellets of $Ce_{0.8-x}Gd_{0.2}Sr_xO_{2-\delta}$ was studied by SEM. A typical micrograph of the surface of the $Ce_{0.78}Gd_{0.2}Sr_{0.02}O_{2-\delta}$ sample is shown in Fig. 2. There are no pores observed on the sample surface, which is consistent with the measured density of the sintered pellet. The mean line intercept technique was used to determine the mean grain sizes. The average grain size of each sample was found to be in the range of 1–3 μm.

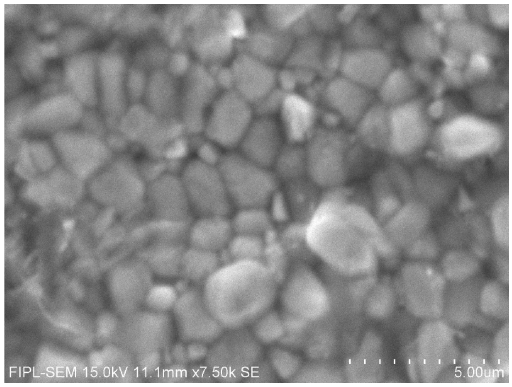

Fig. 2. SEM photograph of the surface of $Ce_{0.8-x}Gd_{0.2}Sr_xO_{2-\delta}$ sintered pellet.

Impedance spectroscopy method is a powerful technique to study the electrical properties of solid electrolytes. Impedance spectroscopy is normally used to separate bulk, grain-boundary and electrode processes in ceramic samples by exhibiting successive semicircles in the complex plane [16]. A high-frequency semicircle originates from the bulk conduction, the lower-frequency semicircle is due to oxide–ion transfer at the surface contact to the electrode, and an intermediate frequency semicircle gives information on the grain-boundary resistance to oxide–ion motion. For each composition impedance data was recorded and for convenience only x = 0.02 composition mentioned here. Figures 3–5 shows an impedance spectrum for $Ce_{0.8-x}Gd_{0.2}Sr_xO_{2-\delta}$ ($x = 0.02$) at different temperatures in the frequency range (0.1 kHz–1 MHz). From Fig. 3 it was observed that spectrum of samples at 350°C, 500°C consists in a semicircle with decreasing bulk resistance (R_b), grain boundary resistance (R_{gb}) and electrode effect (R_e). At 600°C Fig. 4 shows that the spectrum consists of a semicircle and a spike, which indicates that there is no evidence of grain boundary (R_{gb}). As the temperature increases, the bulk semicircle becomes smaller and a depressed circle, a spike exists in the spectra at 700°C (Fig. 5). Spike indicates relatively high oxygen-ion conductivity at higher temperature. The total resistance was then conveniently converted to electrical conductivity (σ) by considering the thickness and area of the sample using Eq. (1).

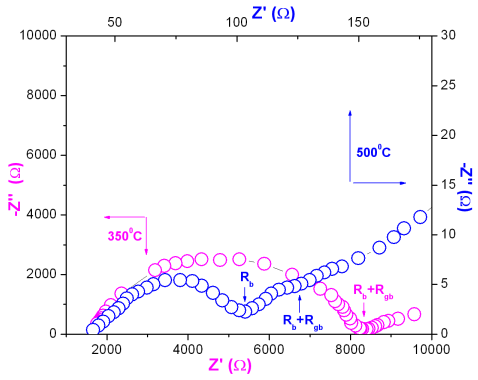

Fig. 3. Impedance spectrum of $Ce_{0.8-x}Gd_{0.2}Sr_xO_{2-\delta}$ ($x = 0.02$) at 350°C and 500°C.

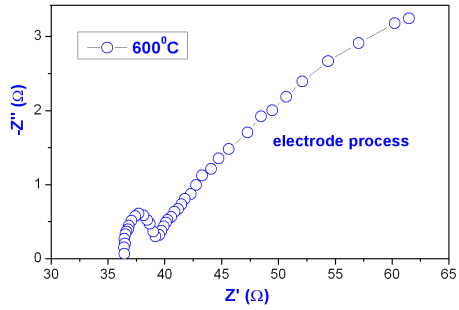

Fig. 4. As in Fig. 3, but for 600°C.

Figure 6 shows the variation of $\log(\sigma T)$ with $1000/T$ for $Ce_{0.8-x}Gd_{0.2}Sr_xO_{2-\delta}$ ($x = 0.0$, 0.02, 0.04, 0.06, 0.08, 0.1) ceramics sintered at 1300°C. The ionic conductivities are significantly enhanced in $Ce_{0.8-x}Gd_{0.2}Sr_xO_{2-\delta}$ ceramic by increasing oxygen vacancies. The ionic conductivity of $Ce_{0.8-x}Gd_{0.2}Sr_xO_{2-\delta}$ decreases with increasing strontium substitution and reaches a maximum for the composition of $Ce_{0.78}Gd_{0.2}Sr_{0.02}O_{2-\delta}$ (0.0236 S/cm) at 700°C compared to that of pure $Ce_{0.8-x}Gd_{0.2}O_{2-\delta}$

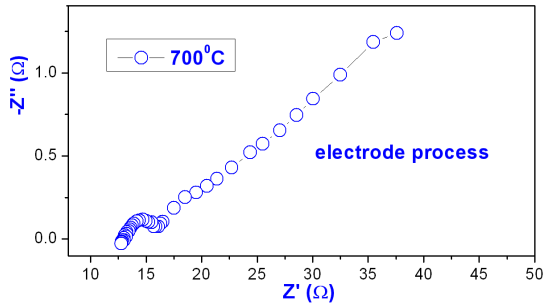

Fig. 5. As in Fig. 3, but for 700°C.

(0.0139 S/cm). The oxide ion mobility increases with increasing temperature, so the conductivity increases, at high temperatures. The activation energy for conduction is obtained by plotting the ionic conductivity data in the Arrhenius relation for thermally activated conduction.

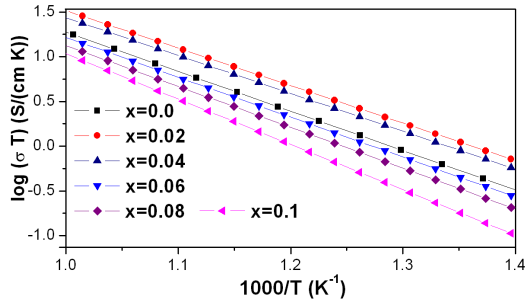

Fig. 6. The temperature dependence of conductivity for $Ce_{0.8-x}Gd_{0.2}Sr_xO_{2-\delta}$.

Figure 7 shows the variation of activation energy as function of Sr doping concentration in $Ce_{0.8-x}Gd_{0.2}Sr_xO_{2-\delta}$ ceramics in the temperature range of 470–700°C. The activation energy is minimum (0.83 eV) for the composition $Ce_{0.78}Gd_{0.2}Sr_{0.02}O_{2-\delta}$. At low dopant concentration ($x = 0.02$), the addition of dopant cation in ceria decreases the activation energy for oxygen vacancy diffusion. This decrease is due to the presence of attractive interactions between dopant cations and oxygen vacancies. Further, increasing the Sr concentration in $Ce_{0.8-x}Gd_{0.2}Sr_xO_{2-\delta}$ ($x = 0.0$, 0.04, 0.06, 0.08, 0.1) system, co-dopant prevents oxygen--ordering leading to higher activation energies and lower oxygen ion conductivity in ceria solid solutions.

Figure 8 shows conductivity (σ [S/cm]) versus doping concentration x at different temperatures. Initially, the total ionic conductivity increases with the increase in dopant concentration. However, it reaches a maximum and drops. The degradation of the total ionic conductivity at higher dopant concentration is related to formation of local defect structures [17], which lowers the mobile oxygen vacancy concentration. The ionic conductivity depends mainly on the mobile oxygen concentration.

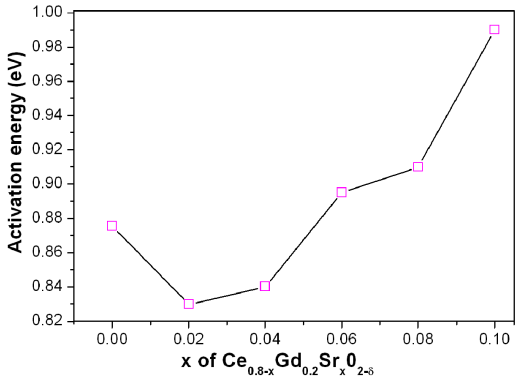

Fig. 7. The variation in activation energy of $Ce_{0.8-x}Gd_{0.2}Sr_xO_{2-\delta}$ of system of specimens.

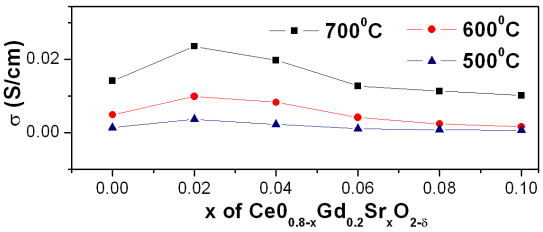

Fig. 8. Composition dependence of total ionic conductivity of $Ce_{0.8-x}Gd_{0.2}Sr_xO_{2-\delta}$ at different temperatures.

4. Conclusions

We have successfully synthesized co-doped ceria samples $Ce_{0.8-x}Gd_{0.2}Sr_xO_{2-\delta}$ ($x = 0.0$, 0.02, 0.04, 0.06, 0.08, 0.1) using the sol-gel method and studied the structure and electrical conductivity in comparison to that of gadolinium doped ceria ($Ce_{0.8}Gd_{0.2}O_{2-\delta}$). The lattice parameter was increased linearly with increasing Sr content. The composition $Ce_{0.78}Gd_{0.2}Sr_{0.02}O_{2-\delta}$ exhibits conductivity over 69% that of $Ce_{0.8}Gd_{0.2}O_{2-\delta}$. For the co-doped ceria samples, ionic conductivities were found to be higher than the singly doped ceria samples. Due to higher ionic conductivity, the present co-doped ceria materials can be used as electrolytes for IT-SOFC applications.

Acknowledgments

One of the authors, S. Ramesh is thankful to UGC, New Delhi for partial financial assistance under the RFSMS scheme.

References

[1] A.S. Arico, A. Sin, E. Kopnin, Y. Dubitsky, A. Zaopo, D. La Rosa, L.R. Gullo, V. Antonucci, *J. Power Sources* **164**, 300 (2007).

[2] I. Riess, *Solid State Ionics* **176**, 1264 (2005).

[3] Z. Tianshu, P. Hing, H. Haung, J. Kilner, *Solid State Ionics* **148**, 567 (2002).

[4] J. Larmine, A. Dicks, *Fuel Cell Systems Explained*, Wiley, London 2000, p. 166.

[5] J.P.P. Huijsmans, *Curr. Opin. Solid State Mater. Sci.* **5**, 317 (2001).

[6] H. Yahiro, Y. Eguchi, K. Eguchi, H. Arai, *J. Appl. Electro-Chem.* **185**, 27 (1988).

[7] B.C.H. Steele, *Solid State Ionics* **129**, 95 (2000).

[8] J. Van Herle, D. Seneviratne, A.J. McEvoy, *J. Eur. Ceram. Soc.* **19**, 837 (1999).

[9] J. Van Herle, T. Horita, T. Kawada, N. Sakai, H. Yokokawa, M. Dokiya, *Solid State Ionics* **86-88** 1255 (1996).

[10] H. Inaba, H. Tagawa, *Solid State Ionics* **83**, 1 (1996).

[11] J.M. Ralph, J. Przydatek, J.A. Kilner, T. Seguelong, *Ber. Bunsenges. Phys. Chem.* **101**, 1403 (1997).

[12] H. Yoshida, H. Deguchi, K. Miura, M. Horiuchi, *Solid State Ionics* **140**, 191 (2001).

[13] T. Mori, J. Drennan, J.H. Lee, J.G. Li, T. Ikegami, *Solid State Ionics* **154-155**, 461 (2002).

[14] H. Yoshida, T. Inagaki, K. Miura, M. Inaba, Z. Ogumi, *Solid State Ionics* **160**, 109 (2003).

[15] R.D. Shannon, *Acta Crystallogr. A* **32**, 751 (1976).

[16] J.E. Bauerle, *J. Phys. Chem. Solids* **30**, 2657 (1969).

[17] H. Yoshida, T. Inagaki, K. Miura, M. Inaba, Z. Ogumi, *Solid State Ionics* **160**, 109 (2003).